

Bonding study of TiC and TiN. II. Theory

P. Blaha, J. Redinger, and K. Schwarz

Institut für Technische Elektrochemie, Technische Universität Wien, A-1060 Vienna, Austria

(Received 29 February 1984)

By starting with self-consistent potentials, the electronic densities and structure factors for stoichiometric TiC and TiN have been calculated with the use of the linearized-augmented-plane-wave (LAPW) method. A comparison is made with the corresponding experimental data which are presented in the preceding paper (Dunand *et al.*), the first paper of this series. Static displacements of titanium occur around nonmetal vacancies in the measured crystals with composition $\text{TiC}_{0.94}$ and $\text{TiN}_{0.99}$. Because of this nonstoichiometry, the experimental data should not be directly compared with theory, which assumes ideal NaCl structure. A sophisticated atomic model introduced in the preceding paper makes it possible to extrapolate to stoichiometric composition. These data are compared with the LAPW results and are found to agree well in the case of TiN and in TiC for the nonspherical effects around Ti; but for TiC, some discrepancies near the nuclei remain which are discussed either in terms of the model parameters used in the fit to experiment or by considering electronic effects caused by vacancies. Chemical bonding is discussed, and it consists of a combination of ionic, covalent, and metallic contributions.

I. INTRODUCTION

Refractory-metal compounds, especially carbides and nitrides, are of particular interest, because on one hand they have high melting points (around 3000 °C) and are ultrahard (comparable to diamond), properties typical of covalent compounds; on the other hand, they are brittle, show metallic luster and metallic conductivity, and some of them (NbC or NbN) are even superconductors with a critical temperature up to 17 K. Many of them crystallize in the NaCl structure—typical for ionic crystals—and since some experiments indicate that there is some charge transfer, these compounds combine covalent, metallic, and ionic binding. This unusual combination of properties makes refractory-metal compounds extremely interesting materials for many special applications.

In the preceding paper,¹ high-precision x-ray-diffraction measurements by Dunand, Flack, and Yvon (denoted DFY below) are presented in which the electron densities for $\text{TiC}_{0.94}$ and $\text{TiN}_{0.99}$ are determined on single crystals. The nonmetal vacancies cause displacements of the Ti atoms with respect to the rocksalt structure; this effect makes it difficult to directly compare the experimental data with theoretical results based on the ideal NaCl structure.

Valvoda and Čapková² have measured the first 10 reflections on powder samples of $\text{TiC}_{0.96}$ using Cu $K\alpha$ radiation. In view of the difficulties in this system, only the much more sophisticated measurements mentioned above will be discussed here.

There are empirical pseudopotential calculations by Alward *et al.*³ which include electron densities, but these have hardly any similarity with the experimental data; thus new investigations are needed.

In this paper we first discuss the bonding mechanism and how it developed over the years (Sec. II); we then discuss the electron densities and structure factors obtained

by linearized-augmented-plane-wave (LAPW) calculations (Sec. III), where accuracy and influence of model parameters are discussed; in Sec. IV comparison with the new experimental data by DFY and their interpretation are presented.

II. BONDING MECHANISM

An experimental situation with such an unusual combination of properties as is found in the refractory-metal compounds is a true challenge to theory. Hägg⁴ was the first to attempt an explanation of these transition-metal compounds involving H, C, N, and O, and he called them “interstitial compounds” because he observed that the metal-metal distance is about the same in the compounds as in the pure metals. Thus he assumed that the nonmetal atoms are deposited in the metal sublattice. The stability requires, from a packing argument, that the ratio of the atomic radii is within the range $0.41 < r_X/r_M < 0.59$.

Rundle⁵ concluded from the increase of the $M-M$ distance (with respect to the pure metal) that a weakening of the $M-M$ bonds occur, since some electrons form $M-X$ σ bonds, which are responsible for the hardness and brittleness of these compounds. Hume-Rothery⁶ followed these ideas, but stressed the importance of the valence-electron concentration.

Krebs⁷ assumed a π bond between p orbitals on X and d orbitals (with t_{2g} symmetry) on M to be essential. Pauling⁸ argued for XM_6 building blocks in which $sp^3d_e^2$ hybridization guarantees covalent bonding.

Bilz⁹ calculated the first band structure for TiC, TiN, and TiO using a simplified LCAO method. He found the $M-X$ bond to be more important than the $M-M$ bond, but, in addition to the covalent aspect, a charge transfer from the metal to the nonmetal takes place.

A large but opposite charge transfer was obtained by Costa and Conte,¹⁰ who completely neglected the $M-X$ in-

teraction. A similar charge transfer from X to M resulted from an empirical LCAO calculation by Lye and Logothetis,¹¹ who adjusted their band structure to optical data. They assumed both $M-M$ and $M-X$ interactions.

There are also authors, such as Samsonov and Uman-skii,¹² Kiessling,¹³ and Dempsey,¹⁴ who favor $M-M$ bonding and disregard the $M-X$ interaction. In this case it is assumed that the nonmetal atoms donate electrons to the $M-M$ metallic bond.

The first *ab initio* band-structure calculation for such compounds was performed by Ern and Switendick,¹⁵ who used the augmented-plane-wave (APW) method. Since their calculation was not self-consistent, their results depend on the choice of starting potential (i.e., the assumed ionicity and atomic configuration). Later, however, Neckel *et al.*¹⁶ showed that self consistent APW calculations agreed in terms of the main features with the early APW work.

Using these APW results, chemical bonding has been discussed in several papers,¹⁶⁻¹⁹ where mainly energy bands and densities of states are used for the analysis, and the reader is referred to review articles (and references therein), one by Calais²⁰ and a very recent one by Neckel.²¹ It is shown in detail that covalent interaction between nonmetal and metal (pd_σ and pd_π) are important, but also $M-M$ bonding (dd_σ) occurs; furthermore, ionic contributions also play a role.

Since in an electron density study charge transfer is an important quantity, it should be mentioned here that even the sign was not clear from the early bonding models. If a superposition of charge densities of the constituent neutral atoms (in their ground states) is taken as reference, then the self-consistent APW calculations^{16,17} clearly yield (e.g., for TiC or TiN) a charge transfer of about half an electron from the metal to the nonmetal, when this difference density (see Fig. 11 of Ref. 17) is integrated over the respective atomic spheres. It should be mentioned that the above reference density corresponds in reciprocal space to what is commonly used in an x-ray-diffraction analysis when atomic form factors are employed to calculate structure factors.

III. ELECTRON DENSITIES AND STRUCTURE FACTORS CALCULATED USING THE LAPW METHOD

Recently, Blaha and Schwarz¹⁷ employed the linearized-APW (LAPW) method to calculate the electron distribution of three representative examples of refractory-metal compounds, namely TiC, TiN, and TiO. This work is based on the self-consistent potentials of the earlier APW results.¹⁶ Since the present paper is an extension of that work, it should be briefly summarized below: Electron densities are used as link between the physicist's band picture and the chemist's bond picture. In Ref. 18 the valence-electron densities of all three compounds are shown, but it is repeated here only for TiC (Fig. 1) as an example. This valence density around C and Ti is comparable in magnitude and is spherically symmetric around carbon, but it is not so around Ti. While p orbitals in a cubic crystal are equally occupied and lead to spherical

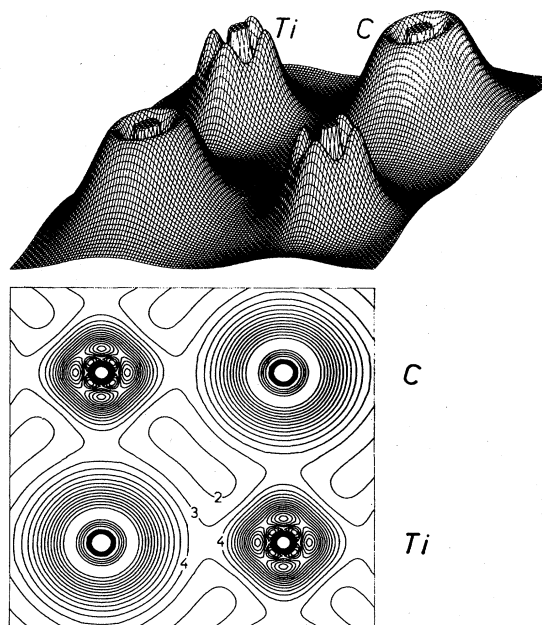


FIG. 1. Theoretical (static) valence-electron density of TiC in the (100) plane obtained by LAPW calculations (Ref. 18). Contour intervals, $0.1e \text{ \AA}^{-3}$, cutoff at $1.7e \text{ \AA}^{-3}$.

symmetry, atomic d orbitals are split in an octahedral crystal field into t_{2g} - and e_g -type orbitals. Only if the ratio between e_g - and t_{2g} -type charges was 2:3, as is that of their degeneracies, a spherical symmetric density would result. The actual LAPW valence-electron densities show that for TiC the e_g component dominates (Figs. 1 and 2), for TiN a slight t_{2g} excess is found, but for TiO, t_{2g} clearly dominates. These observations have been traced back to features in the corresponding band structures or partial densities of states.¹⁶

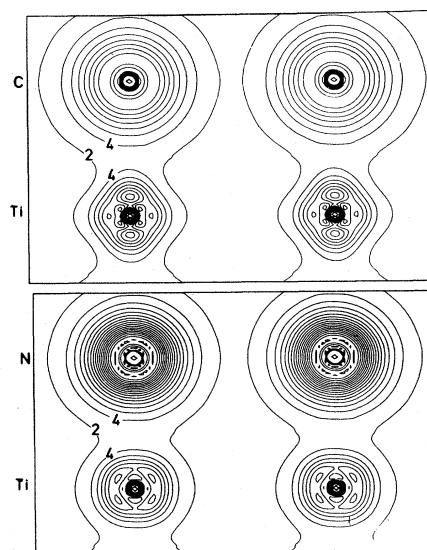


FIG. 2. Theoretical valence-electron density of TiC and TiN in the $(1\bar{1}0)$ plane. Contour intervals, $0.2e \text{ \AA}^{-3}$; values in units of $0.1e \text{ \AA}^{-3}$.

A. LAPW formalism for structure factors

In the LAPW formalism the unit cell is broken down into atomic spheres and a region outside these spheres where wave functions and, consequently, the corresponding electron densities are expressed differently. In both regions the contribution to the structure factor is defined as a Fourier transform (FT) of the density.

For the present case the density *inside atomic sphere* p (with radius R_p) can be written in terms of radial functions $C_L^M(r)$ multiplied by cubic harmonics K_L^M (which are linear combinations of spherical harmonics),

$$\rho(\vec{r}) = \sum_{L,M} C_L^M(r) K_L^M(\hat{r}), \quad (1)$$

where the $C_L^M(r)$ are derived from valence (and semicore) LAPW wave functions by means of a projection operator according to Ref. 18; a FT gives

$$f_{\vec{K}}^p = 4\pi \sum_{L,M} i^L K_L^M(\hat{K}) \int_0^{R_p} C_L^M(r) j_L(Kr) r^2 dr, \quad (2)$$

where the j_L are spherical Bessel functions. *Outside* the atomic spheres (i.e., the plane-wave region in LAPW), the density is given as Fourier series,

$$\rho(\vec{r}) = \sum_{\vec{K}'} \rho_{\vec{K}'} \sum_{R \in G_{\vec{K}'}} \exp(i\vec{K}' \cdot \underline{\mathbf{R}}^{-1} \cdot \vec{r}), \quad (3)$$

where R denotes a symmetry operation (and $\underline{\mathbf{R}}$ its matrix representation) of the point group $G_{\vec{K}'}$. The FT yields

$$f_{\vec{K}}^{\text{out}} = \Omega \sum_{\vec{K}'} \rho_{\vec{K}'} \sum_{R \in G_{\vec{K}'}} \delta(\vec{K}' \cdot \underline{\mathbf{R}}^{-1} \cdot \vec{K}) - 4\pi \sum_p R_p^2 \times \begin{cases} R_p/3, & \vec{K}'' = \vec{0} \\ \exp(i\vec{K}'' \cdot \vec{r}_p) \frac{j_1(|K''| R_p)}{|K''|}, & \vec{K}'' \neq \vec{0} \end{cases} \quad (4)$$

with $\vec{K}'' = \vec{K}' \cdot \underline{\mathbf{R}}^{-1} - \vec{K}$; Ω is the volume of the unit cell. With these definitions the total structure factor is given by

$$F_{\vec{K}} = f_{\vec{K}}^{\text{out}} + \sum_p f_{\vec{K}}^p \exp(i\vec{K} \cdot \vec{r}_p). \quad (5)$$

In calculations of structure factors, three aspects should be emphasized which are often treated differently in various methods: (i) relativistic effects, (ii) treatment of exchange and correlation, and (iii) the frequently used muffin-tin approximation.

Recently, Schneider²² discussed various calculations of structure factors for copper and compared them with experimental data. MacDonald *et al.*²³ performed LAPW calculations including relativistic and non-muffin-tin corrections. They employed two types of exchange and correlation potentials, one of $X\alpha$ type with $\alpha = \frac{2}{3}$ (exchange only) and the other using the local-density approximation by Gunnarsson *et al.*²⁴ The two calculations yield very similar results which also agree well with early (nonrelativistic, muffin-tin, $X\alpha$) APW calculations by

Snow *et al.*²⁵ High-precision measurements for Cu using γ -ray diffractometry have been performed by Schneider *et al.*,²⁶ and absolute structure factors which agree to within about 0.8% with the theoretical values were obtained. In a compound the muffin-tin radii should be chosen such that the smallest discontinuities in the potentials and the charge densities appear between the atomic spheres. It was demonstrated for VC that even drastic variations in the radii cause only small changes in the electron densities.²⁷

The present examples show that relativistic, muffin-tin, and exchange-correlation effects play only a minor role in calculating structure factors. An accuracy of about 1% can be assumed for the present theoretical models.

B. LAPW structure factors of TiC and TiN

Using the formalism described in the preceding subsection, we calculated structure factors for TiC and TiN (Table I) with a normalization of one formula unit per unit cell. (A complete list can be obtained from the authors.) In these calculations one can use several approximations, especially for the core states. The calculation marked F_{LAPW} was done using LAPW densities for the valence (X 2s, 2p and Ti 3d) and the semicore (Ti 3s, 3p) states, and atomic densities derived from the self-consistent field (SCF) crystal potentials for the core (X 1s and Ti 1s, 2s, 2p) states; this is called the thawed-core approximation. In the present work these structure factors are thought to be the most reliable because all states are calculated from crystalline data using a consistent model. For TiC the influence of various approximations on this model is shown in Table I (columns a–c) as the differences $F_{\text{LAPW}} - F_i$, where valence contributions cancel.

(a) We neglect the \vec{k} dependence of the Ti-semicore states and calculate atomic scattering factors for Ti 3s and 3p states using the respective SCF crystal potentials. This simplification affects the 111 reflection by only 0.1%, and the deviation further decreases with rising $(\sin\theta)/\lambda$.

(b) The effect of the often used “frozen-core” approximation is demonstrated in column b. Only the valence structure factors are derived from band theory, but all others are calculated from atomic wave functions using the $X\alpha$ method. Differences of up to 0.5% can be found, and even at high scattering vectors small deviations from the “thawed-core” model exist. This can be traced back mainly to the semicore states which differ between SCF crystal and atomic potential.

(c) Using a Hartree-Fock (HF) frozen-core model for core and semicore states leads to differences (column c) of up to 0.5% at higher $(\sin\theta)/\lambda$ values. Crystallographers commonly use atomic HF scattering factors taken from Fukamachi²⁸ and the International Tables.²⁹ They implicitly assume that core and semicore densities remain atomiclike and, therefore, are well described by such a procedure, but all solid-state effects come from valence states only. This last assumption, however, is not completely fulfilled, as can be seen from column b, of Table I where, within the $X\alpha$ scheme, core and semicore states are different in the atomic or crystalline case. For the

TABLE I. Calculated structure factors for TiC and TiN normalized to one formula unit per unit cell. The method of computation for valence, semicore, and core states is indicated at the bottom. Columns a–c are differences $F_{LAPW} - F_i$, where for F_i semicore and core are treated as indicated; column d gives the effect of two lattice constants (a complete listing can be obtained from the authors).

<i>h</i>	<i>k</i>	<i>l</i>	$(\sin\theta)/\lambda$ (\AA^{-1})	F_{LAPW}	TiC				TiN
					a	b	c	d	F_{LAPW}
0	0	0	0.0000	28.000	0.000	0.000	0.000	0.000	29.000
1	1	1	0.2001	-12.000	0.015	0.042	0.033	0.001	-10.934
2	0	0	0.2311	18.383	-0.002	-0.031	-0.020	-0.004	19.143
2	2	0	0.3268	14.813	-0.006	-0.028	-0.006	-0.004	15.263
3	1	1	0.3832	-9.193	0.003	0.018	-0.015	0.003	-8.570
2	2	2	0.4002	12.741	-0.008	-0.021	0.003	-0.004	13.029
4	0	0	0.4621	11.558	0.001	-0.006	0.016	-0.004	11.612
3	3	1	0.5036	-7.400	0.002	0.004	-0.027	0.003	-7.063
4	2	0	0.5167	10.599	-0.001	-0.004	0.014	-0.003	10.659
4	2	2	0.5660	9.916	-0.001	-0.002	0.011	-0.003	9.981
5	1	1	0.6003	-6.506	-0.001	-0.002	-0.027	0.002	-6.201
3	3	3	0.6003	-6.433	0.000	-0.001	-0.026	0.002	-6.221
4	4	0	0.6535	9.019	0.000	0.000	0.003	-0.002	9.062
5	3	1	0.6835	-5.897	-0.000	-0.003	-0.019	0.002	-5.687
4	4	2	0.6932	8.682	0.000	0.000	-0.002	-0.002	8.738
6	0	0	0.6932	8.747	0.001	0.001	-0.001	-0.002	8.710
6	2	0	0.7307	8.450	0.001	0.002	-0.005	-0.002	8.445
5	3	3	0.7576	-5.504	0.000	-0.002	-0.011	0.001	-5.330
6	2	2	0.7663	8.194	0.001	0.002	-0.009	-0.002	8.213
4	4	4	0.8004	7.936	-0.001	-0.001	-0.015	-0.002	8.004
5	5	1	0.8251	-5.233	-0.000	-0.002	-0.007	0.001	-5.048
7	1	1	0.8251	-5.271	-0.001	-0.002	-0.007	0.001	-5.031
13	5	5	1.7097	-2.450	0.000	0.002	-0.009	0.002	-2.203
11	7	7	1.7097	-2.447	0.001	0.002	-0.009	0.002	-2.204
12	8	4	1.7291	3.402	-0.000	-0.003	-0.001	-0.003	3.456
Valence				$X\alpha$ LAPW	$X\alpha$ LAPW	$X\alpha$ LAPW	$X\alpha$ LAPW		$X\alpha$ LAPW
Semicore				$X\alpha$ LAPW	$X\alpha$ thawed	$X\alpha$ frozen	HF frozen	$\Delta F_{X\alpha}^{\text{atom}}$	$X\alpha$ LAPW
Core				$X\alpha$ thawed	$X\alpha$ thawed	$X\alpha$ frozen	HF frozen	$a_{\text{theor}} - a_{\text{expt}}$	$X\alpha$ thawed

first reflections a comparison between column b and c indicates that the frozen-core approximation dominates over the difference between the $X\alpha$ and HF approximations.

(d) Since the experimentally obtained lattice constant¹ for TiC (4.329 65 \AA) differs by 0.04% from the one used in theory (4.327 76 \AA), we have examined its effect by calculating atomic $X\alpha$ structure factors for these two lattice parameters. The differences given in column d of the table were found to be small and are at most 0.1% at higher $(\sin\theta)/\lambda$.

For TiN the situation is quite similar to TiC and therefore only F_{LAPW} is presented.

In summary, one can say that the influence of different core models (HF, $X\alpha$, frozen or thawed core) should affect structure factors by less than 0.5%. In the preceding paragraph we discussed, for Cu, that relativistic effects, the muffin-tin approximation, or different exchange-correlation potentials influence structure factors by not more than 1%.

C. Convergence of Fourier synthesis

Valence-electron densities (as shown in Figs. 1 and 2) can be calculated directly using the LAPW formalism ac-

ording to Eqs. (1) and (2). From such a density, structure factors are obtained according to Eqs. (2), (4), and (5). A Fourier synthesis allows us to recalculate the density, which agrees well with the directly obtained values, except near the nucleus, where deviations occur. The latter are caused by the cutoff in $(\sin\theta)/\lambda$ corresponding to a finite number of reflections (123 in the present case).

The convergence of the Fourier synthesis is illustrated in Fig. 3, where valence densities in the (100) plane around the Ti atom are shown which are derived from structure factors with four different cutoff windows. Originating from Ti 3*d* functions, four maxima corresponding to e_g symmetry can be seen. The peak maximum and its distance from the nucleus decrease when the window is shifted to larger values of $(\sin\theta)/\lambda$. Near the nucleus the density contribution changes from negative in the first two pictures to positive in the last two, and reflects the radial nodal structure of the Ti 4*s* function. The fact that even for the highest window the *d* peak is still present and the maximum near the nucleus is very high, clearly illustrates that valence densities are not fully converged, even if structure factors up to $(\sin\theta)/\lambda = 1.73 \text{\AA}^{-1}$ are included.

Atomic HF scattering factors are shown in Fig. 4 for an analysis of this situation in reciprocal space. Looking

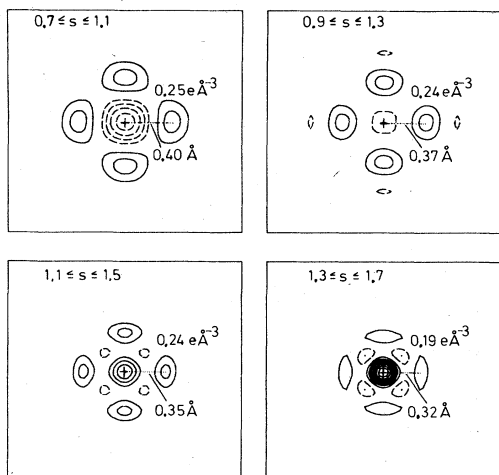


FIG. 3. Valence-electron density of TiC around the titanium atom in the (100) plane as a function of the cutoff window for $s = (\sin\theta)/\lambda$. The calculations are based on the LAPW structure factors; the density at the peak maximum and its distance from the nucleus are specified in each case: Positive contours, solid line; negative contours, dashed line.

at the core and valence decomposition of the form factor [Fig. 4(a)], one would assume that valence contributions to the structure factor should be negligible for $(\sin\theta)/\lambda \geq 0.6 \text{ \AA}^{-1}$. This crude picture, however, must be wrong considering the poor convergence of the valence density described above, but this can be understood from Fig. 4(b), where the valence-orbital contributions (normalized to unity) to the atomic form factor are shown on a very fine scale. Although these contributions become small beyond 0.5 \AA^{-1} , they are not negligible since there is a large number of such reflections (six reflections below 0.5 \AA^{-1} , but more than 100 between 0.5 and 1.7 \AA^{-1}). Therefore measurements at high $(\sin\theta)/\lambda$ values should still contain information about the valence densities in these compounds, although its experimental detection could be complicated by thermal motion. The high Debye tem-

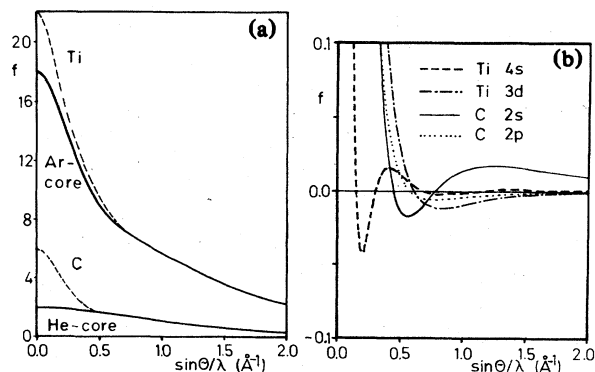


FIG. 4. Atomic form factors of Ti and C from the Hartree-Fock calculations (Ref. 28 and 29): (a) the total and the (Ar or He) core contributions, and (b) orbital form factors (normalized to unity) for all valence states; the decrease from 1 to 0.1 is not shown.

peratures, however, suggest that the dynamical effects could be sufficiently well described in these systems. Note that this poor convergence is also the reason why a plane-wave expansion of the total crystal wave function is not sufficient and one must augment the plane-wave basis set (e.g., the APW method).

IV. COMPARISON WITH EXPERIMENTAL DATA

A. Rudimentary model

In the first paper of this series by Dunand, Flack, and Yvon¹ (DFY), the results of a high-precision, high-resolution x-ray-diffraction study on nonstoichiometric crystals of composition $\text{TiC}_{0.94}$ and $\text{TiN}_{0.99}$ have been presented. A usual refinement of the experimental data, correcting for extinction and thermal vibration, and treating nonstoichiometry by occupancy factors only, yields difference densities as shown in Figs. 1 and 2 of DFY. For TiC, a strong deviation from spherical symmetry around the titanium site is found which leads to maxima of $1.41e \text{ \AA}^{-3}$ along the $\langle 100 \rangle$ directions and to minima of $-0.85e \text{ \AA}^{-3}$ along the $\langle 111 \rangle$ directions.

In the present paper, this situation is shown in the form of the theoretical valence-electron densities (Fig. 2). The nonspherical effects are in qualitative agreement with the experiments, namely spherical symmetry around carbon and maxima around titanium in the $\langle 100 \rangle$ directions. A quantitative comparison, however, shows that, in theory, the nonspherical effect is significantly smaller than that according to this first analysis of the experimental data. Instead of showing the theoretical difference densities, we can simply count the contour lines from the minima in the $\langle 111 \rangle$ directions to the maxima in the $\langle 100 \rangle$ directions, and estimate this difference to be about $1e \text{ \AA}^{-3}$, while experiment yields about $2.3e \text{ \AA}^{-3}$.

This discrepancy in direct space can also be analyzed in reciprocal space, where nonspherical effects can be investigated by structure factors of equal length, i.e., $|\vec{K}_1| = |\vec{K}_2|$, so-called paired reflections. If the density can be described by a superposition of spherically symmetric atomic densities, paired reflections should have the same value, i.e., they are independent of the direction of their corresponding scattering vectors. Otherwise, the weighted difference of paired reflections,

$$F = (F_1 - F_2)/G, \quad (6)$$

where G is a geometrical factor defined by DFY, is a measure for the deviation from spherical symmetry.

In TiC, such a nonspherical effect is present, which originates from the Ti 3d electrons and is evident from the paired reflections (Fig. 5). The LAPW results show that the nonspherical effects in terms of ΔF clearly decrease (although slowly) with $(\sin\theta)/\lambda$, while the experimental ΔF values drastically increase. As discussed by DFY in connection with their Fig. 11, this situation cannot originate from an electronic effect only, but a static displacement of the titanium atoms caused by the carbon vacancies can account for this increase in ΔF . If the experimental data (solid line of Fig. 5) are corrected for ΔF corresponding to these displacements (dashed line of Fig. 5),

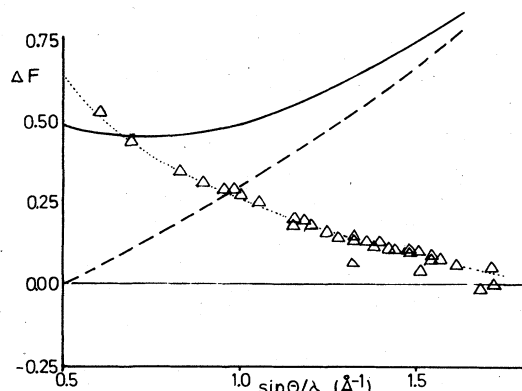


FIG. 5. Nonspherical effects in TiC derived from paired reflections according to Eq. (6): LAPW results (triangles), effect of static displacements (dashed line), and the curve through experimental data (solid line) are taken from DFY (Ref. 1).

good agreement with the present calculation is obtained.

The slow decrease of the theoretical ΔF values with $(\sin\theta)/\lambda$ shows that the valence form factor (Ti 3d in this case) contributes appreciably to the nonspherical effect even for large values of $(\sin\theta)/\lambda$. In this context it is interesting to observe a similar slow decrease of the Ti 3d form factor [Fig. 4(b)].

B. Sophisticated model

In the rudimentary model described above, non-stoichiometry has been treated only by occupancy factors, but this is insufficient, at least in the case of $\text{TiC}_{0.94}$. The shortcoming of this simple model comes from neglecting the displacements of the titanium atoms. Before a detailed comparison between theory and experiment can be made, a model is needed which on one hand reproduces the experimental data sufficiently well, but on the other allows us to go over to an ideal crystal assumed by theory; i.e., stoichiometric composition, no displacements, static (no thermal vibrations), and extinction free.

Such a model has been developed by DFY and is described in detail in their paper. It consists of an atomic model with partial orbital occupancies p , κ parameters controlling the expansion or contraction of the valence form factors, harmonic thermal vibrations, and non-stoichiometry effects. The latter are described by occupation parameters ϵ_X of nonmetal (X), metal (M), and displaced metal (D) sites, assuming that around each X vacancy the six neighboring metal atoms are displaced by x_D along the $[100]$ direction, where the same scattering factors are used for both types of titanium atoms. DFY accurately fitted their experimental data and obtained a set of parameters given in their Tables I and II.

Assuming that all the parameters are not only fitting parameters but that they have physical significance, we can calculate static structure factors of an ideal crystal, denoted $F_c^{1.0}$, which are derived from the experimental data. For this purpose we set ϵ_X and ϵ_{Ti} to unity to achieve stoichiometry; then we keep the titanium orbital occupancies, but renormalize the nonmetal values in order

to guarantee electroneutrality. This renormalization going from $\text{TiC}_{0.94}$ to $\text{TiC}_{1.0}$ changes the carbon orbital occupancies as follows: $p_{\text{He}}, 2.0 \rightarrow 1.97$; $p_{2s}, 3.07 \rightarrow 3.02$; $p_{2p}, 3.11 \rightarrow 3.05$. In the following discussion the structure factors $F_c^{1.0}$ and the corresponding densities will be referred to as "experimental results," but it should be pointed out that the above model is used as link to transfer the experimental data from the real crystal to the ideal one.

We are now in a position where we can compare experimental and theoretical results, since both should correspond to an ideal crystal. The difference densities derived from $F_c^{1.0} - F_{\text{LAPW}}$ (Fig. 6) shows generally good agreement for TiN judging by the many (dashed) zero lines; for TiC, however, significant positive densities around both atoms are observed, indicating a stronger localization in experiment than in theory. The nonspherical effects agree well in all cases since the residual densities are almost spherically symmetric around each atom.

The valence charge density obtained by the empirical pseudopotential method³ for TiC yields a spherically symmetric density around titanium but small nonspherical effects around carbon, contrary to experiment. Since only d functions, and not p functions, are split in an octahedral environment (crystal field), deviations from spherical symmetry can only occur around Ti.

Another analysis of these deviations can also be made in reciprocal space by comparing the structure factors $F_c^{1.0}$ with F_{LAPW} [Fig. 7(a)]. The differences between them ($|F_c^{1.0}| - |F_{\text{LAPW}}|$), especially for smaller $(\sin\theta)/\lambda$ values, are much larger for TiC than for TiN.

For TiN the differences $|F_c^{1.0}| - |F_{\text{LAPW}}|$ are small and always less than 1%, except for the 111 reflection.

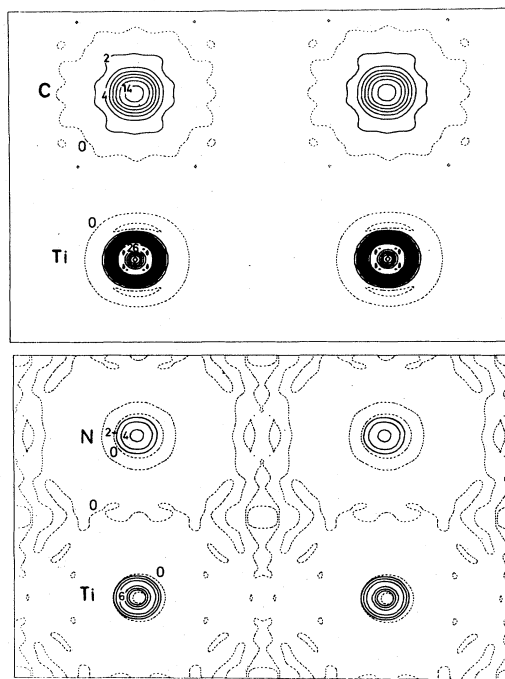


FIG. 6. Difference density in the $(1\bar{1}0)$ plane for TiC and TiN obtained from $F_c^{1.0} - F_{\text{LAPW}}$ of the valence electrons. Contour intervals, $0.2e \text{ \AA}^{-3}$; values in units of $0.1e \text{ \AA}^{-3}$.

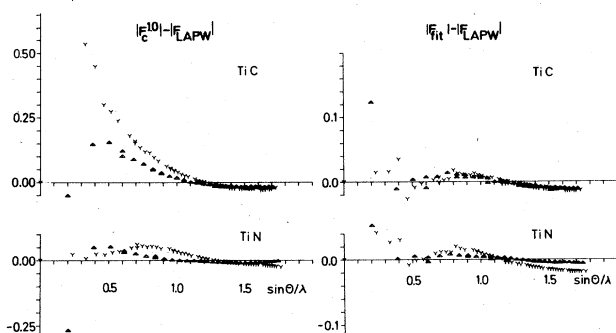


FIG. 7. Difference in structure factors for TiC and TiN for even (Y) and odd (Δ) reflections, where F_{fit} is taken from Ref. 30: (a) between experiment (model) and theory (LAPW), i.e., $|F_c^{1.0}| - |F_{\text{LAPW}}|$; (b) between fit (using same model as above) and theory (LAPW), i.e., $|F_{\text{fit}}| - |F_{\text{LAPW}}|$.

Considering the experimental error bars and the uncertainties introduced by some approximations in theory, the agreement is excellent.

For TiC, however, deviations up to 4% occur, where even reflections ($h+k+l=2n$) corresponding to $F=f_{\text{Ti}}+f_{\text{C}}$ differ from the odd reflections with $F=f_{\text{Ti}}-f_{\text{C}}$. This different behavior between even and odd reflections can be understood if we assume that both f_{Ti} and f_{C} derived from experiment are greater than the respective quantities from theory, because then partial cancellation can take place for odd reflections but not for even.

In order to know whether the differences shown in Fig. 7(a) are tolerable or not, the same fitting procedure which was applied to the raw experimental data was also used by Dunand and Flack³⁰ to fit the theoretical (LAPW) structure factors, and the results shall be denoted F_{fit} . The deviations of F_{LAPW} [Fig. 7(b)] are small and indicate that

the basis functions used in the fitting procedure are sufficiently flexible to reproduce the theoretical data well.

Although this is difficult to see from Fig. 7(a), it should be mentioned that the differences of paired reflections (as discussed in connection with Fig. 5) in the sophisticated model of $F_c^{1.0}$ show a decrease with $(\sin\theta)/\lambda$ quite similar to that in F_{LAPW} . Therefore, the contributions from static displaced titanium atoms seem to be properly treated.

Let us return to direct space and examine the corresponding density differences, where one-dimensional plots are sufficient, since the residual densities are spherically symmetric. While for TiN the difference density between experiment and theory [Fig. 8(a)] is of the same order of magnitude as deviations between the fit and theory [Fig. 8(b)], for TiC the deviations near the atoms are significantly larger for the experimental density than for the fit case. A similar argument holds for deviations in reciprocal space by comparing Fig. 7(a) with 7(b).

C. Parameters of the sophisticated model

In the preceding subsection concerning the sophisticated model, two types of fits have been discussed—one which fits the experimental data of the real crystal ($\text{TiC}_{0.94}$ and $\text{TiN}_{0.99}$) and one which attempts to reproduce the theoretical structure factors F_{LAPW} using the same atomic model, which we denoted $(\text{TiC})_{\text{fit}}$ and $(\text{TiN})_{\text{fit}}$. Table II lists the essential parameters of these fits, additional details being given by DFY.

As a first step, the orbital occupancies p_i are analyzed and comparisons between fit, APW, and experiment are made.

(i) The p_{4s} in the fit cases are much greater than the respective values of about $0.13e$ obtained in the APW calculations.¹⁶ This discrepancy can be understood by considering that, in the APW formalism, these values correspond to $4s$ -like charges which lie inside the titanium

TABLE II. Parameters obtained by a nonlinear least-squares fit of structure factors of TiC and TiN. The values in the columns headed $(\text{TiC})_{\text{fit}}$ and $(\text{TiN})_{\text{fit}}$ denote the fit (Ref. 30) to the LAPW structure factors (where a constant $\sigma=0.0025$ was taken, assuming a normalization per formula unit), while the fit to experiment taken from DFY (Ref. 1) is given in the columns headed $\text{TiC}_{0.94}$ and $\text{TiN}_{0.99}$.

	$(\text{TiC})_{\text{fit}}$	$\text{TiC}_{0.94}$	$(\text{TiN})_{\text{fit}}$	$\text{TiN}_{0.99}$
λ_X	1.00	0.94	1.00	0.99
x_D		0.097		
p_{4s}	1.20(13)	0.44(40)	1.20(10)	1.09(38)
$p_{t_{2g}}$	0.72(03)	0.76(04)	1.00(04)	0.65(05)
p_{e_g}	0.80(03)	0.75(04)	0.51(03)	0.35(04)
p_{2s}	1.28(09)	3.07(37)	1.17(11)	1.81(65)
p_{2p}	4.01(19)	3.11(63)	5.12(17)	5.12(66)
κ_{4s}	1.01(05)	0.94(10)	1.00(05)	0.91(06)
$\kappa_{t_{2g}}$	1.18(03)	1.77(08)	1.14(03)	1.40(08)
κ_{e_g}	1.10(03)	1.47(07)	1.17(05)	1.42(12)
κ_{2s}	0.99(03)	0.97(05)	0.90(03)	0.78(08)
κ_{2p}	0.92(02)	1.20(09)	0.95(01)	0.96(06)
$Q(\text{Ti})$	1.29(13)	2.05(39)	1.29(11)	1.91(37)
R (%)	0.16	0.25	0.16	0.23

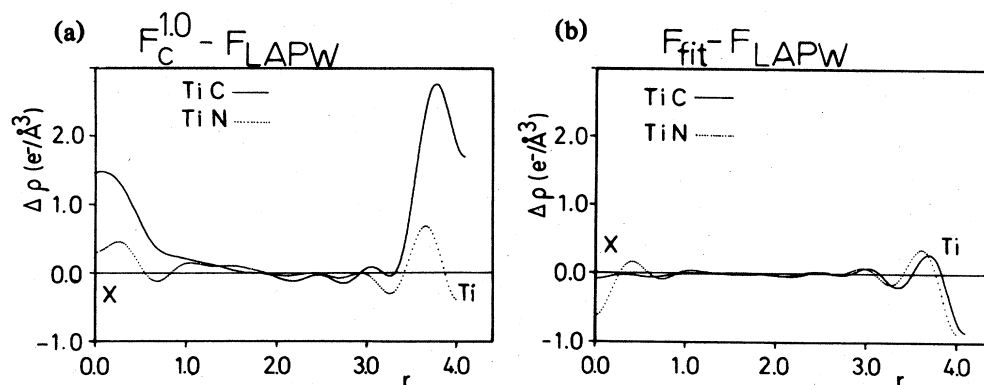


FIG. 8. Difference density in the [100] direction for TiC and TiN using data for $(\sin\theta)/\lambda < 1.73 \text{ \AA}^{-1}$: (a) with $F_C^{1.0} - F_{LAPW}$ [one-dimensional cut in Figs. 6(a) and 6(b)]; (b) with $F_{fit} - F_{LAPW}$.

spheres, but most of the charge originating from Ti 4s wave functions is found outside the atomic spheres, where the APW method yields more than two electrons. In contrast to this spatial division of charge, the fit corresponds to a linear combination of atomic orbitals picture where the orbital occupancies specify how much charge is centered at the corresponding atomic site. For a discussion of this fundamental differences between APW and LCAO, see, for example, Ref. 18. While, for TiN, fit and experiment are comparable, for TiC a much smaller value is found in experiment, but the very large standard deviation (σ) should be noted.

(ii) The ratio between $p_{t_{2g}}$ and p_{e_g} , important for the nonspherical effects, agrees well between fit and experiment; it is about 1:1 for TiC and 2:1 for TiN. While in the former case the absolute values also agree, in TiN the entire d -like charge is about $0.5e$ smaller in experiment. The LAPW results¹⁸ show trends similar to the fit case since (in contrast to the $4s$ -like charge) the $3d$ -like charge is rather localized inside the titanium sphere.

(iii) The nonmetal occupancies p_{2s} and p_{2p} in $\text{TiC}_{0.94}$ cannot have too much physical significance, since the value of 3.07 for p_{2s} is clearly greater than 2, the physically given limit. The increasing localization from carbide to nitride leads to a slight increase of p_{2s} in APW calculations,¹⁶ but here a decrease is found.

(iv) The net atomic charge $Q(\text{Ti})$ clearly indicates a charge transfer from Ti to the nonmetal, but these quantities are directly affected by the uncertainties in the orbital occupancies. The fact that the charge transfer obtained in the APW calculations¹⁶ is smaller, and only about $0.4e$ again comes from the LCAO versus spatial partitioning of charge, as discussed above for the $4s$ -orbital occupancies.

In the second part of this discussion the κ parameters which are used in the fitting model to allow the orbitals to expand or contract are analyzed. These parameters should give additional flexibility for the basis functions to describe solid-state effects. For that purpose the orbital scattering factors for the solid at $(\sin\theta)/\lambda = s$ are taken from the free atom at s/κ . Table II shows that some κ parameters remain close to 1, but values such as 1.77 or 0.78 also occur. These values are certainly too large

(small) and may result from shortcomings in the DFY model (for example, the thermal vibrations of the 36% displaced Ti atoms are assumed to be isotropic, and both types of titanium atoms have the same form factors, i.e., $f_D = f_{Ti}$). Such values which differ significantly from 1.0 dramatically alter the orbital form factors f_{nl} shown in Fig. 4(b); e.g., a κ of 1.77 shifts the intersection of f_{3d} with the abscissa from 0.6 to about 1.0 \AA^{-1} . For the atom, f_{3d} is already very small at $s = 1.77 \text{ \AA}^{-1}$, but at $s/\kappa = 1.0 \text{ \AA}^{-1}$ a relatively large f_{3d} is effective and leads to poorly converged densities.

For an additional analysis of the effects of κ parameters, we have calculated structure factors with our atomic model that we have simplified by setting all orbital occupancies equal to zero, except that corresponding to the Ti 3d orbital, where we assume that $p_{t_{2g}} = 0.6$ and $p_{e_g} = 0.4$ in order to generate a spherically symmetric density around the Ti site. Densities obtained from these structure factors are shown in Fig. 9 and allow us to investigate the influence of various κ values in direct space. The

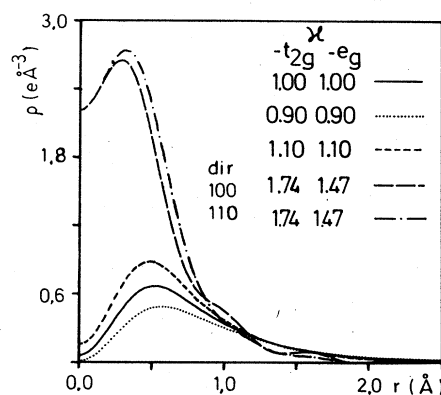


FIG. 9. Effect of the κ parameter on the density around a Ti atom; a model density is used which consists of one d electron on Ti in a NaCl lattice ($p_{t_{2g}} = 0.6$ and $p_{e_g} = 0.4$). If, for t_{2g} and e_g , equal κ values are used, spherical symmetry remains; otherwise the density is shown in both the [100] and the [110] directions.

solid curve corresponding to $\kappa=1.0$ is the reference state derived from free atomic data and shows the typical shape of a $3d$ density, and the small value at the Ti origin indicates good convergence—if structure factors up to 1.73 \AA^{-1} are used. A uniform change of κ by ± 0.1 leads to a small contraction or expansion, but the main effect is a change in the peak height. Using the experimental κ values of 1.77 and 1.47 for t_{2g} - and e_g -symmetry components, the corresponding densities are more localized around the titanium atom and their peak maximum is nearly 4 times as large as in the $\kappa=1$ case. The resulting density does not resemble a Ti $3d$ density, and therefore the change caused by such κ values goes far beyond solid-state effects. Functions of that type lose their physical significance and play the role of almost arbitrary fitting functions. Judged by the very large values at the origin, we see that convergence is not achieved even if structure factors up to $(\sin\theta)/\lambda=1.73 \text{ \AA}^{-1}$ are used. Furthermore, spherical symmetry around the Ti site is lost, as can be seen from Fig. 9 where densities in the [100] and [110] directions are plotted. From this example it is evident that the assumed spherical symmetry can only be recovered if the different κ values for t_{2g} and e_g are compensated for by their respective orbital occupancies, a fact which illustrates the correlation between these parameters.

In this context it is important to consider that there is an energy dependence of the Ti $3d$ wave functions. If states with mainly t_{2g} or e_g symmetry fall in different energy regions, then the radial part of the corresponding electron densities of the two symmetries could differ. However, such an effect would be small in the present cases and should appear mainly in the tail region and not near the $3d$ maximum, where the κ values are most effective. Consequently, the κ values of the two symmetries should be about the same (and near unity), a requirement which is almost satisfied in TiC_{fit} and TiN_{fit} (Table II).

V. DISCUSSION AND CONCLUSION

In this paper the LAPW method was used to calculate electron densities and the corresponding structure factors. As discussed in Sec. III, relativistic effects, non-muffin-tin corrections, the use of various exchange-correlation potentials, or different treatments of core and semicore states should affect the structure factors by less than 1%. An analysis of the present results has shown that even at $(\sin\theta)/\lambda$ values as high as 1.7 \AA^{-1} , *valence* states contribute to structure factors, and therefore measurements should be carried out to such high scattering lengths.

A quantitative comparison between theory and x-ray-diffraction measurements is performed in Sec. IV. A usual refinement of the experimental data (rudimentary model) was insufficient, especially in the case of $\text{TiC}_{0.94}$, where the carbon vacancies require a more elaborate treatment of nonstoichiometry than that using occupancies only.

In order to overcome these difficulties, DFY have employed a sophisticated atomic model which has the advantage over the often used multipole model that it is based more on physics than on mathematics. This model should bring us into a better position to do the difficult job of

transferring data from the experiment, carried out on a real crystal, to the ideal situation as assumed by theory. The following requirements of the model must be satisfied in order to succeed.

(i) The model should be sufficiently flexible to reproduce the experimental data well.

(ii) It should allow us to extrapolate from the experimental conditions to an ideal crystal, i.e., stoichiometric composition, with neither static nor dynamic displacements, and without extinction. In order to satisfy this condition, we require that all parameters used in this model represent properly, but also exclusively, the physical phenomenon for which they have been introduced.

(iii) Electronic effects caused by vacancies should play a negligible role, so that keeping the atomic form factors unchanged when going from the defect case to the stoichiometric one is justified.

DFY have shown with their sophisticated model that the experimental data are reproduced well, and thus the first requirement is satisfied.

The extrapolated data agree well with theory in the case of TiN, while for TiC, discrepancies remain that are larger than the estimated error bars (of both experiment and theory). A further analysis has shown that for TiC the nonspherical components of the electron density agree well with theory and the effects of the displaced titanium atoms seem to be included correctly in the model. The discrepancies in TiC are found in the electron densities near the atoms, where experiment (i.e., the extrapolation to $\text{TiC}_{1.0}$) yields significantly higher values than theory. A similar situation occurs for the small-angle reflections with deviations up to 4%.

The origin of these discrepancies indicates that the other two requirements may not be strictly fulfilled. DFY have found several correlations between parameters, and, here, the correlation between κ and p_i parameters was discussed above. Furthermore, since some atomic functions are drastically distorted by high values (1.77 for Ti $3d$), and occupancies outside their quantum-mechanical limits appear (p_{2s} for carbon), the physical significance of the model is, to some extent, lost.

The other possibility could be that the carbon vacancies introduce true electronic effects which alter the electron density in such a way that a simple extrapolation to stoichiometric composition is no longer possible. From the present results, a quantitative analysis of such effects cannot be made, but formation of "vacancy bands" have been reported in literature, for example, in the defect structure of NbO .³¹

In the two papers of this series it is demonstrated that vacancies drastically affect the electron densities of compounds, although the deviation from stoichiometry is only a few percent. This observation is not surprising if one considers that around each carbon vacancy at least the six nearest-neighbor titanium atoms will be displaced (i.e., in $\text{TiC}_{0.94}$, about 36% of the titanium atoms). The present investigations have once more shown the enormous importance of sample preparation and characterization, especially in the context of a comparison with theory, where ideal crystals are normally assumed.

Apart from the difficulties caused by defects, theory

and experiment are in good agreement and they lead to the following bonding picture.

(i) There is a clear charge transfer from the metal to the nonmetal, but the amount depends on the model used to define this charge transfer (Mulliken versus spatial partitioning). This establishes the ionic component of the bonding.

(ii) The covalent pd_σ bonds become evident in TiC in terms of nonspherical effects (with e_g symmetry) of the electron density. Such a bonding, although weaker, is also present in TiN, but in contrast to TiC, more Ti $3d$ orbitals with t_{2g} symmetry are occupied that form dd_σ and pd_π bonds; thus in TiN an overall almost spherically symmetric density around Ti results, but this does not imply that covalency is absent.

(iii) Metallic bonding can be discussed more easily in terms of densities of states than by electron densities, in which the energy dependence is lost. Conductivity measurements or band theory, however, clearly show that metallic bonding must be present.

Since the chemical bonding in these compounds consists of a combination of ionic, covalent, and metallic contributions, the early binding mechanisms were able to give some explanation, although often only one aspect was considered to be important. In such a complicated bonding situation no quantitative statement about ionic, covalent, or metallic contributions can be made, since these terms are only defined in idealized cases.

It should be pointed out that the collaboration between

theory and experiment was particularly fruitful in this investigation, since, for example, the attempt to compare data from the real crystal with theory led us to carefully analyze the vacancy problem. Other theories^{3,11,32} come to different conclusions, and, therefore, it was important to confirm the present theory by experiment. Another argument is best illustrated for TiN, where experimental data lead to an almost spherically symmetric density around Ti, from which it would be difficult to derive a bonding mechanism, but, since the LAPW results agree well with this observation, theory allows a further analysis by considering contributions from various energy regions separately,¹⁸ a procedure which is inaccessible to x-ray diffraction.

Recently, Trebin and Bross³² calculated the electron density of TiC and obtained a dominance of t_{2g} symmetry around Ti, in contrast to the present result. This discrepancy, however, was explained by Blaha *et al.*³³ and could be traced back to an overly restricted \vec{k} summation used in their density calculation.

ACKNOWLEDGMENTS

The calculations have been performed at Interfakultäres Rechenzentrum der Technischen Universität Wien. This work was partly supported by the Hochschuljubiläumstiftung der Stadt Wien. We thank Dr. A. Dunand and Dr. H. D. Flack for performing the non-linear least-squares fit on the LAPW structure factors.

¹A. Dunand, H. D. Flack, and K. Yvon, preceding paper [Phys. Rev. B **31**, 2299 (1985)].

²V. Valvoda and P. Čapková (unpublished).

³J. F. Alward, C. Y. Fong, M. El-Batanouny, and F. Wooten, Solid State Commun. **17**, 1063 (1975).

⁴G. Hägg, Z. Phys. Chem. B **12**, 33 (1931).

⁵R. E. Rundle, Acta Crystallogr. **1**, 180 (1948).

⁶W. Hume-Rothery, Philos. Mag. **44**, 1154 (1953).

⁷H. Krebs, Acta Crystallogr. **9**, 95 (1956).

⁸L. Pauling, *The Nature of the Chemical Bond*, 3rd ed. (Cornell University Press, Ithaca, 1960).

⁹H. Bilz, Z. Phys. **153**, 338 (1958).

¹⁰P. Costa and R. R. Conte, in *Compounds of Interest in Nuclear Reactor Technology*, edited by J. T. Waber, Institute of Metals Division, Special Report No. 13 (Edwards, Ann Arbor, Michigan, 1967).

¹¹R. G. Lye and E. M. Logothetis, Phys. Rev. **147**, 622 (1966).

¹²G. V. Samsonov and Ya. S. Umanskii, NASA Tech. Transl. **F102** (1962).

¹³R. Kiessling, Metall. Rev. **2**, 77 (1957).

¹⁴E. Dempsey, Philos. Mag. **8**, 285 (1963).

¹⁵V. Ern and A. C. Switendick, Phys. Rev. **137**, 1927 (1965).

¹⁶A. Neckel, P. Rastl, R. Eibler, P. Weinberger, and K. Schwarz, J. Phys. C **9**, 579 (1976); British Library Supplementary Publication Scheme SUP70017.

¹⁷A. Neckel, K. Schwarz, R. Eibler, P. Weinberger, and P. Rastl, Ber. Bunsenges. Phys. Chem. **79**, 1053 (1975).

¹⁸P. Blaha and K. Schwarz, Int. J. Quant. Chem. **XXIII**, 1535 (1983).

¹⁹K. Schwarz and P. Blaha, in *Local Density Approximation in Quantum Chemistry and Solid State Physics*, edited by J. P. Dahl and J. Avery (Plenum, New York, 1984), p. 605.

²⁰J. L. Calais, Adv. Phys. **26**, 847 (1977).

²¹A. Neckel, Int. J. Quantum Chem. **XXIII**, 1317 (1983).

²²J. Schneider, Fortschr. Mineral. **61**, 85 (1983).

²³A. H. MacDonald, J. M. Daams, S. H. Vosko, and D. D. Koelling, Phys. Rev. B **25**, 713 (1982).

²⁴O. Gunnarsson, B. I. Lundqvist, and J. W. Wilkins, Phys. Rev. B **10**, 1319 (1974).

²⁵E. C. Snow and J. T. Waber, Phys. Rev. **157**, 570 (1967).

²⁶J. Schneider, N. K. Hansen, and H. Kretschmer, Acta Crystallogr. Sect. A **37**, 711 (1981).

²⁷K. Schwarz, K. Pechter, and A. Neckel, J. Phys. C **8**, 1663 (1975).

²⁸T. Fukamachi, Institute of Solid State Physics (ISSP) Report No. **B12**, University of Tokyo, 1971 (unpublished).

²⁹*International Tables for X-ray Crystallography* (Kynoch, Birmingham, 1974), Vol. IV.

³⁰A. Dunand and H. D. Flack (unpublished).

³¹E. Wimmer, K. Schwarz, R. Podloucky, P. Herzig, and A. Neckel, J. Phys. Chem. Solids **43**, 439 (1982).

³²H.-R. Trebin and H. Bross, J. Phys. F **14**, 1453 (1984).

³³P. Blaha, K. Schwarz, and J. Redinger, J. Phys. F (to be published).